

The Toll/NF- κ B signaling pathway is required for epidermal wound repair in *Drosophila*

Lara Carvalho^{a,b}, António Jacinto^{a,b}, and Nina Matova^{a,1}

^aInstituto de Medicina Molecular, Edifício Egas Moniz, 1649-028 Lisbon, Portugal; and ^bCentro de Estudos de Doenças Crónicas, NOVA Medical School/Faculdade de Ciências Médicas, Universidade Nova de Lisboa, 1169-056 Lisbon, Portugal

Edited by Trudi Schüpbach, Princeton University, Princeton, NJ, and approved November 3, 2014 (received for review May 28, 2014)

The Toll/NF- κ B pathway, first identified in studies of dorsal-ventral polarity in the early *Drosophila* embryo, is well known for its role in the innate immune response. Here, we reveal that the Toll/NF- κ B pathway is essential for wound closure in late *Drosophila* embryos. Toll mutants and *Dif dorsal* (NF- κ B) double mutants are unable to repair epidermal gaps. Dorsal is activated on wounding, and Dif and Dorsal are required for the sustained down-regulation of E-cadherin, an obligatory component of the adherens junctions (AJs), at the wound edge. This remodeling of the AJs promotes the assembly of an actin-myosin cable at the wound margin; contraction of the actin cable, in turn, closes the wound. In the absence of Toll or *Dif* and *dorsal* (*dl*), both E-cadherin down-regulation and actin-cable formation fail, thus resulting in open epidermal gaps. Given the conservation of the Toll/NF- κ B pathway in mammals and the epithelial expression of many components of the pathway, this function in wound healing is likely to be conserved in vertebrates.

Toll pathway | NF- κ B transcription factors | epithelial wound repair | *Drosophila* | E-cadherin

The epidermis, the outermost layer of cells, protects the animal body from adverse environmental agents, prevents water loss, and provides mechanical resistance in organisms as diverse as insects, worms, and humans. Epidermal integrity is maintained at all times and wounds are repaired efficiently through resealing of the broken edges.

A prominent mechanism for wound repair involves the assembly of an actin cable in the epidermal cells bordering the lesion (1, 2). The actin cable is contractile: Its circumference rapidly diminishes as the epidermal gap shrinks in size. While the actin cable contracts, the cells around the wound elongate, move and come together from all sides, thus restoring the epidermal continuum. This mechanism is termed a “purse-string” wound closure and is documented in a number of species including *Drosophila*, *Caenorhabditis elegans*, *Xenopus*, zebrafish, chick, mouse, and human (3).

The molecular mechanisms that control epidermal wound repair are not well understood. The transcription factors Grainy head and Jun are required for wound repair both in *Drosophila* and the mouse (3–6). However, the interplay between transcription and the cytoskeletal structures that execute wound closure has not been investigated. Previously, we showed that two *Drosophila* NF- κ B transcription factors, Dif and Dorsal, are required for the integrity of the larval epidermis (7). Although single *Dif* or *dl* mutants do not have a detectable epidermal phenotype, *Dif dl* double-mutant larvae have spontaneous epidermal lesions and systemic infection by microbes from the environment (8). Expression of *dl* in the epidermis of *Dif dl* animals rescues the epidermal defects. Tissue-specific epidermal expression of *dl* also prevents the infection, indicating that the lesions in *Dif dl* larvae compromise the barrier function of the epidermis.

In *Drosophila*, the NF- κ B/I κ B complex mediates signaling from the Toll receptor and the Toll/NF- κ B pathway is best understood in gastrulation (9). In the early embryo, Toll is activated by Spätzle (10, 11). Toll signal transduction leads to the proteolysis of Cactus, the *Drosophila* I κ B, and to the translocation of

the NF- κ B protein Dorsal to the nucleus (12–14). The cells that receive the highest level of Toll signaling reorganize their apical adherens junctions (AJs) and assemble a contractile actin cable at their apical sides (15, 16). Contraction of the actin cable creates a fold in the embryo known as the ventral furrow. There, the prospective mesodermal cells will ingress in the embryo. Thus, all events that encompass gastrulation are governed by Toll activation.

Members of the Toll/NF- κ B pathway remain expressed in the epidermis in later stages of *Drosophila* embryogenesis and in larvae, pupae, and adults (17–19) (modENCODE and this report). Later in development, a second NF- κ B protein, Dif, is expressed and overlaps in function with Dorsal (8, 20, 21).

Toward the end of embryogenesis (stages 15–17), the *Drosophila* epidermis is a simple epithelium consisting of a single layer of cells. Mature junctional complexes connect the epithelial cells: The subapical complex, AJs, and septate junctions are all present and required for proper epidermal structure (22). An essential component of the AJs is E-cadherin, a transmembrane protein that mediates cell-to-cell adhesion and, in association with β -catenin and α -catenin, links the adhesion complex to F-actin.

Here, we show that wound repair in the late embryonic epidermis depends on the Toll/NF- κ B pathway. On wounding, E-cadherin is rapidly down-regulated in cells surrounding the lesion; this event is followed by actin polymerization and the placement of bundles of F-actin at the membrane of the cells bordering the gap. After epidermal wounding of Toll mutants and *Dif dl* double mutants, both E-cadherin down-regulation and actin-cable formation fail. The data show that Toll pathway acts in two ways. Dif and Dorsal control the initial, fast phase in E-cadherin remodeling in epidermal cells. Photobleaching experiments indicate

Significance

Injury and repair of broken skin are an integral part of human existence, but the ability to heal wounds extends across species. Animals ranging from insects and worms to fish, amphibians, birds, and mammals all protect and restore body integrity. Our study reveals that the evolutionary-conserved Toll/NF- κ B signaling pathway, which provides the first line of defense against microbial infection, is crucial for wound repair in the embryonic epidermis (the skin) of the insect *Drosophila melanogaster*. Toll/NF- κ B signaling promotes remodeling of cellular junctions and assembly of a cytoskeletal ring around the wound. Contraction of this ring much like a “purse string” fastens the epidermal gap. The findings set the stage for a similar investigation of the pathway in wound repair in vertebrates.

Author contributions: N.M. designed research; L.C. and N.M. performed research; L.C., A.J., and N.M. analyzed data; L.C. and N.M. prepared figures; N.M. wrote the paper; and N.M. conceived and supervised the project.

The authors declare no conflict of interest.

This article is a PNAS Direct Submission.

¹To whom correspondence should be addressed. Email: nina.matova@aya.yale.edu.

This article contains supporting information online at www.pnas.org/lookup/suppl/doi:10.1073/pnas.1408224111/-DCSupplemental.

that the Toll/NF- κ B pathway promotes rapid E-cadherin turnover at the wound site. Later in wound closure, activity of the Toll/NF- κ B pathway leads to transcriptional repression of *E-cadherin* in the cells bordering the wound, and this second activity likely contributes to the continuous down-regulation of E-cadherin during epithelial resealing. Our findings suggest that the Toll/NF- κ B signaling module is a stress sensor that is activated robustly during tissue damage. The damage-induced transcriptional output not only restores epidermal integrity, it also prepares the epidermis to respond to subsequent injuries and other stress-related events.

Results

***Toll*^{-/-} Mutants and *Dif dl* Double Mutants Are Unable To Close Epidermal Wounds.** We showed that the NF- κ B genes, *Dif* and *dl*, are important for epidermal integrity (7), but their mechanism of action was not clear. The larval epidermis of the double mutants appeared to have normal morphology; therefore, the lesions in the epidermis of *Dif dl* larvae could not be easily related to defects in epidermal development. Instead, we favored the hypothesis that epidermal lesions arose because of defective healing of wounds that occur normally during the lifespan of the animal (7). The previous experiments were done in larvae, which are well suited for immunity studies as they are in constant contact with the environment. To study wound repair, we chose to look at the late embryonic epidermis because embryos move less, can be wounded in a controlled manner, and imaged live for several hours after wounding.

We created wounds by laser ablation of a patch of epidermal cells in the ventral epidermis of late embryos of stages 15 and 16 following an established protocol (23). Wound closure was scored and the percentage of unclosed wounds was calculated 16 h later. Although the vast majority of the control *w¹¹¹⁸* embryos (92.5%, *n* = 157) closed the epidermal lesions, wounds remained open in 65.3% (*n* = 87) of *Dif dl* injured animals (Fig. 1 *A* and *D*). Similarly, 70.3% (*n* = 64) of the *Toll*^{-/-} embryos were unable to repair inflicted epidermal wounds (Fig. 1 *C*).

Previous statistical analysis defined 30% open wounds as the cutoff threshold, which separates reliably mutants with wound-healing defects from controls (23). Therefore, we observed a clear wound-repair phenotype in *Toll*^{-/-} mutants and in *Dif dl* double

mutants. Compared with reported results (23), the percentage of unclosed wounds places *Toll*^{-/-} and *Dif dl* among the mutants with the strongest wound-repair defects.

Because Spätzle is the ligand that activates Toll in early embryos, we wounded *spätzle* (*spz*) null embryos. Our scoring indicated that *spz* embryos had 15.8% open wounds (*n* = 143). Thus, the wound-healing defect in *spz* mutants falls well below the defined threshold and is more similar to the controls (Fig. 1 *A* and *B*). Maternal contribution of Spz that could lead to rescue seems unlikely: The maternal Spz proteins decrease sharply at 5–6 h after egg laying (stage 10 of embryogenesis) and are hardly detectable on a Western blot (10). We suggest that during epidermal repair, Spätzle is not the principal ligand that triggers Toll activation.

Continuous Actin Cable Fails To Assemble in Wounded Embryos Lacking Toll/NF- κ B Activities. Repair of embryonic epidermal wounds does not involve cell division; instead, it is accomplished through cytoskeletal remodeling and cell-shape changes (24). A central event following injury is the assembly of the supracellular actin cable around the gap (2). The actin cable is believed to be important in two ways: Initially, it stabilizes the wound edge of the broken epidermis and, subsequently, it contracts, thus providing the force for gap closure (25). Because the cable is the most prominent structure that appears de novo at the wound edge, we investigated the ability of *Toll*^{-/-} mutants and *Dif dl* double mutants to build actin cable after wounding.

In control embryos (*w¹¹¹⁸*), a continuous actin cable is assembled gradually between 5 and 15 min after ablation around an epidermal wound of approximately 2,800 μ m² and remains visible almost until the gap disappears, approximately 2–3 h after wounding. Using phalloidin staining, we examined the actin cable in controls (*n* = 18) at 2 h after wounding (Fig. 2 *A*) when the embryos were in the final stages of wound closure. The cable was still robust and spanned the entire circumference of the wound (Fig. 2 *A*, *A'*, and *A''*). At the same time, we stained the embryos with E-cadherin antibody to visualize the AJs in the epidermis (Fig. 2 *B*). We observed that epidermal cells in controls lacked E-cadherin at the wound edge (Fig. 2 *A'''*, arrowheads). Similar findings were reported earlier (25) and, together with our observations, demonstrate that the cells bordering the gap remodel their AJs after wounding.

We then investigated wounded *spz* embryos (*n* = 8). Resembling the controls, these mutant embryos displayed strong and continuous actin cable (Fig. 2 *C*, *C'*, and *C''*) and lacked E-cadherin at the membranes facing the wound (Fig. 2 *C'''*, arrowheads).

By contrast, neither *Toll*^{-/-} nor *Dif dl* mutants (*n* = 10 for each genotype) had a continuous actin cable around the gap at 2 h after wounding (Fig. 2 *E* and *G*). Delicate bundles of F-actin in the epidermal cells around the wound were interspersed with regions where no actin bundles could be seen. Unlike wild-type embryos, E-cadherin was present at the membrane in *Toll*^{-/-} (Fig. 2 *E'*, *E''*, and *E'''*, arrow) and in *Dif dl* (Fig. 2 *G'*, *G''*, and *G'''*, arrows) epidermal cells that lacked an actin cable at the wound edge. However, mutant epidermal cells that assembled some actin bundles had little or no E-cadherin staining on the membranes that faced the wound (Fig. 2 *E'*, *E''*, and *E'''*, arrowhead). Thus, in *Toll*^{-/-} and *Dif dl* embryos, F-actin and E-cadherin had a mutually exclusive localization pattern at the membranes facing the gap.

To rule out the possibility that a cable was built in the mutants but disassembled earlier in the process, we examined embryos at 30 min and at 1 h after wounding. At no time point did we see a continuous actin cable around the epidermal gap in *Dif dl* mutants. We also examined the localization of the nonmuscle Myosin II in controls and in *Dif dl* mutants after wounding (Fig. S1). Whereas control embryos localized Myosin II along the entire circumference of the actin cable, *Dif dl* animals showed Myosin II only in cells that had built actin bundles at the wound edge and

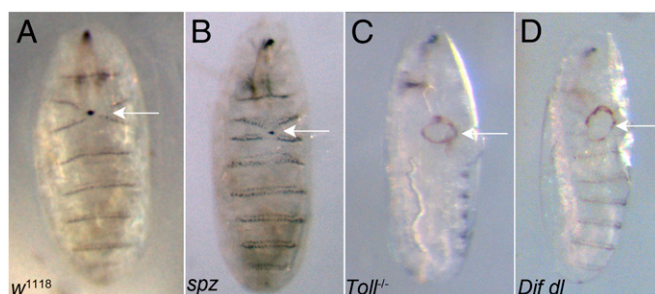


Fig. 1. Defects in epithelial repair in *Toll*^{-/-} and *Dif dl* mutant embryos following laser ablation. (*A*) Controls (*w¹¹¹⁸*) closed inflicted epidermal lesions in 92.5% of the tested embryos (*n* = 157). Arrow points to a closed wound. (*B*) Wounded *spz* embryos were able to close wounds in the ventral epidermis in 84.2% of the tested mutants (*n* = 143). Arrow shows a closed wound. (*C*) *Toll*^{-/-} embryos failed to close experimentally introduced wounds in 70.3% of the tested mutants (*n* = 64). Arrow points to an open epidermal gap. (*D*) *Dif dl* mutants did not close wounds after laser ablation of a patch of the ventral epidermis in 65.3% of the tested embryos (*n* = 87). Arrow marks the open wound. Although ablation is always done ventrally, after 16 h of recovery, the open wound could be found on the lateral side in *Toll*^{-/-} and *Dif dl* mutants. The number of embryos for each genotype constitutes the combined counts from six to nine independent wounding sessions. The *Toll* transallelic combination represents a strong loss-of-function phenotype; *Dif dl* double mutants and *spz* mutants represent a null phenotype.

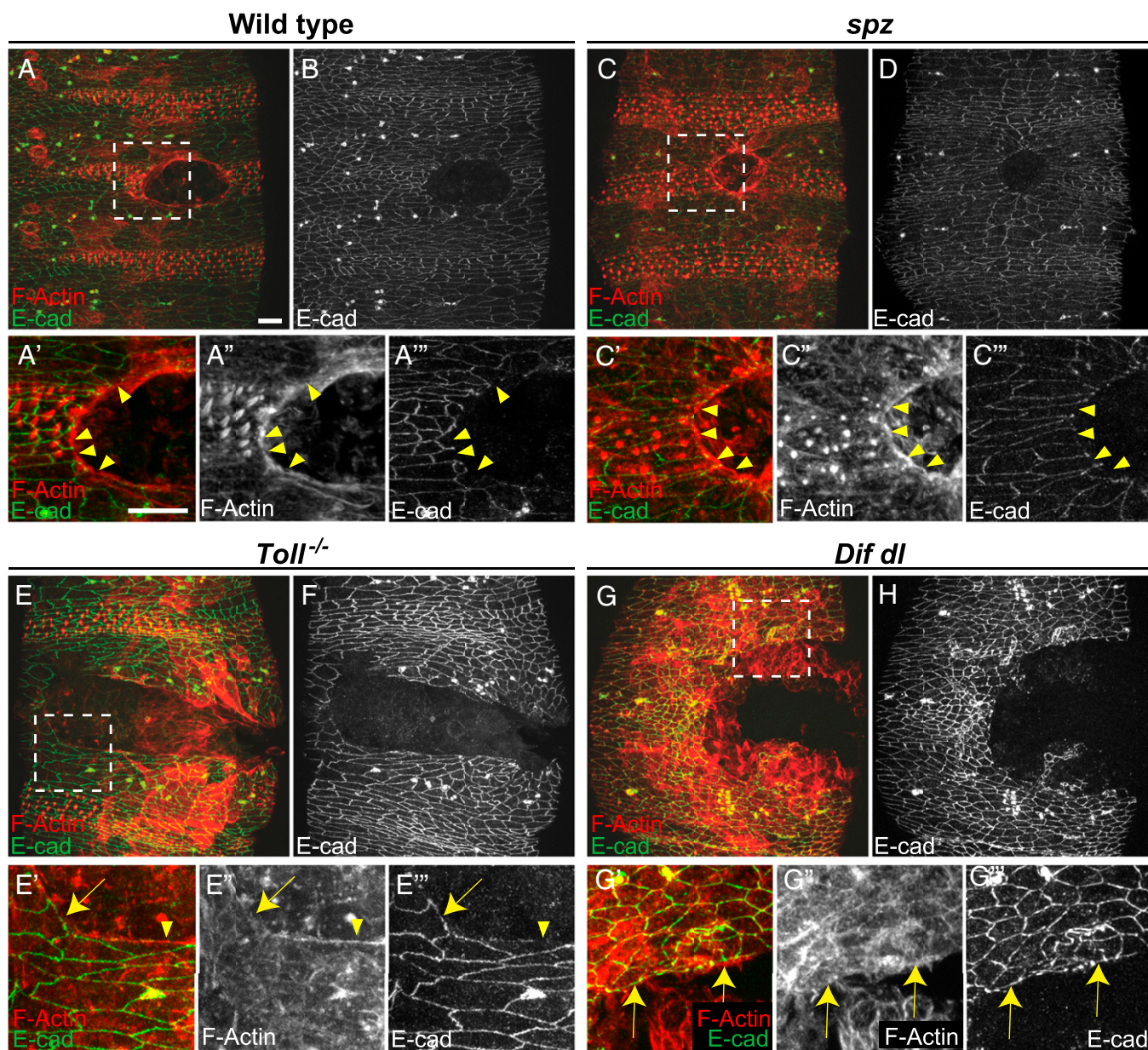


Fig. 2. Wounded *Toll*^{-/-} mutants and *Dif dl* double mutants do not build a continuous actin cable. Embryos of stage 15 were stained for F-actin (phalloidin) and E-cadherin at 2 h after wounding. (A, C, E, and G) are merged images, whereas (B, D, F, and H) show only E-cadherin. Identical settings were used for all images. Areas for the close-ups are outlined by squares in A, C, E, and G. (A, A', A'', A''', and B) In wild type, wound-edge cells are contracting and the wound is closing. Wound-edge epidermal cells show a continuous actin cable (A' and A''). E-cadherin (B and A''', arrowheads) is excluded from the membranes facing the wound. (C, C', C'', C''', and D) In *spz* embryos, wound-edge cells are contracting and wound closure is similar to wild type. Wound-edge cells have a continuous actin cable (C' and C''). E-cadherin (D and C''', arrowheads) is not present at the membranes that face the wound. (E, E', E'', E''', and F) In *Toll*^{-/-} embryos, the actin cable is discontinuous. Epidermal cells that maintain high levels of E-cadherin at the membranes bordering the gap (E''', arrow) do not assemble an actin cable (E' and E'', arrow). In wound-edge cells where some actin bundles are assembled (E' and E'', arrowhead), E-cadherin is reduced at the membranes facing the gap (E''', arrowhead). (G, G', G'', G''', and H) In *Dif dl* embryos, the actin cable is discontinuous. Epidermal cells that maintain high levels of E-cadherin at the membranes bordering the gap (G''', arrows) do not assemble an actin cable (G' and G'', arrows) at the wound margin. (Scale bars: 10 μm.) Images are the maximum z projections of 11.1- to 22-μm stacks (30–55 slices). Close-ups are the maximum z projections of 5.2- to 18.4-μm stacks (14–46 slices).

not in cells that lacked bundles. Thus, Myosin II followed closely the interrupted pattern of F-actin bundles in *Dif dl* embryos.

We concluded that the building of continuous and contractile actin cable, the most striking event in wound repair, requires the Toll/NF-κB pathway.

Dynamic Junctional Remodeling After Wounding Is Impaired in *Dif dl* Mutants. The results showed that the cells bordering the wound remodel E-cadherin (and their AJs) in the aftermath of epidermal

injury. Because E-cadherin remained at the wound edge in *Toll*^{-/-} and in *Dif dl* embryos, we hypothesized that Toll/NF-κB signaling is involved in the reorganization of E-cadherin in wound-edge epidermal cells.

To investigate the dynamics of E-cadherin localization at a cellular resolution after wounding, we performed live imaging of wound closure in the epidermis. We used an *E-cadherin::GFP* (*E-cad::GFP*) transgene that was expressed under the control of the *ubiquitin* promoter (*ubi-E-cad::GFP*). The fusion protein,

E-cad::GFP, is fully functional as previously demonstrated (26). We used a membrane-tethered mCherry Fluorescent Protein (membrane::mCherry) expressed under the control of the *spaghetti squash* promoter to visualize the wound edge (*sqh-Gap43::mCherry*) (27).

In wild-type embryos (*ubi-E-cad::GFP/+*), the epidermal cells of the wound edge down-regulated E-cad::GFP as early as 5 min after wounding (Fig. 3 *A* and *B*, arrows and *Movie S1*). The changes in E-cad::GFP were fast and slightly asynchronous: All cells would remove E-cad::GFP from the wound edge membrane

but that occurred seemingly independently in each cell that bordered the wound. The rapid loss from the wound-edge cells was followed by the formation of E-cad::GFP foci in the lateral plane of the wound-edge cells (Fig. 3*B*, arrowheads). A continuous actin cable formed later and was clearly visible at 15 min after wounding (*Movie S2*).

By contrast, cells at the wound edge in *Dif dl* mutants showed high levels of E-cad::GFP at 5 min after wounding (Fig. 3 *E* and *F*, arrows). An optical cross section (YZ) through the wound margin confirmed that the fluorescence dropped in wild-type

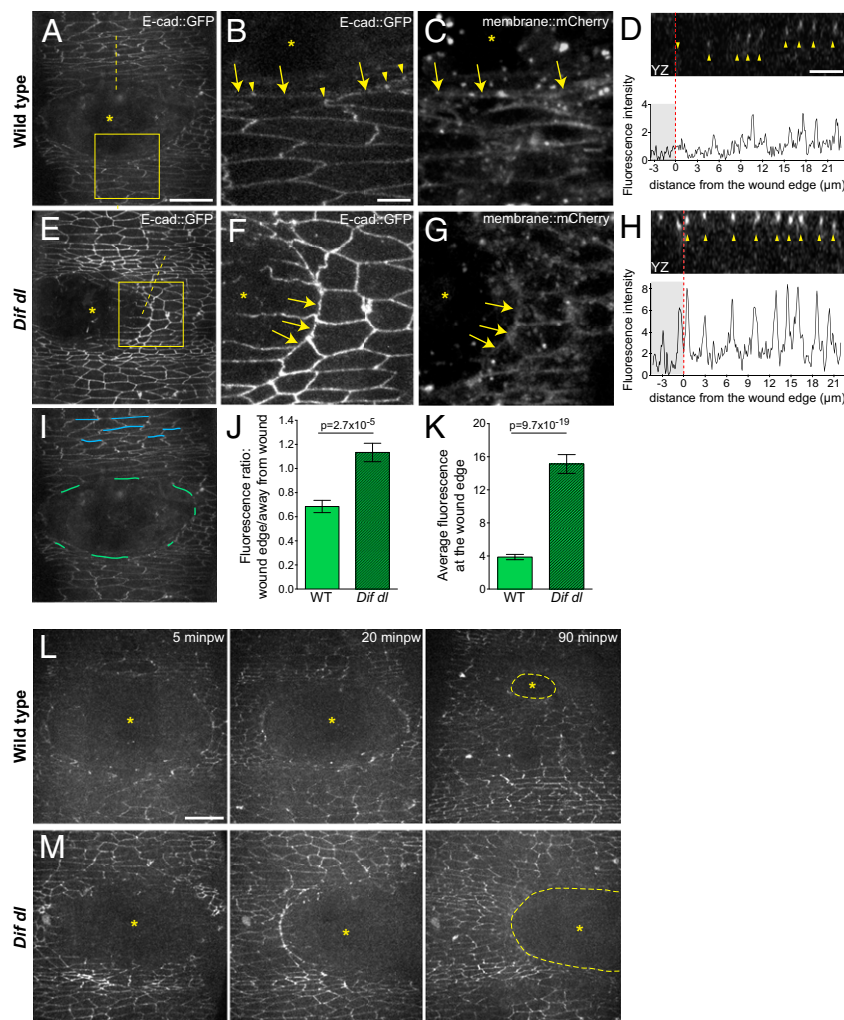


Fig. 3. Remodeling of E-cad::GFP at the wound edge fails in *Dif dl* mutants. (*A–H*) Ventral epidermis of embryos at stage 15 expressing E-cad::GFP and membrane::mCherry. *A*, *B*, *D–F*, and *H* show E-cad::GFP, whereas *C* and *G* show membrane::mCherry. Images are taken with identical settings at 5 min after wounding of wild type (*A–D*) and *Dif dl* (*E–H*). (*B*, *C*, *F*, and *G*) are high-magnification images of the wound edge in wild-type and *Dif dl* embryos (boxed regions in *A* and *E*). In wild type, wound-edge membranes have low levels of E-cad::GFP (*A*; *B*, arrows) compared with cellular junctions at a distance from the wound. In wound-edge cells, E-cad::GFP is present as apical puncta (*B*, arrowheads) at contact points between the cells. In *Dif dl*, all epidermal cells, at the wound edge and far from the wound, have high levels of E-cadherin (*E*; *F*, arrows). Wound-edge membranes are outlined by membrane::mCherry (*C* and *G*). Asterisks mark the wound. (*D* and *H*) YZ cross sections of the epidermis (apical side is up). Dashed lines in *A* and *E* mark the positions of the cross-sections. The graphs show the fluorescence intensity profiles of E-cad::GFP in these YZ cross-sections. The wound area is shaded; the wound margin is marked with a red dashed line. Both wild-type and *Dif dl* embryos display apical localization of E-cad::GFP (arrowheads in *D* and *H*). Wild-type cells have low levels of E-cad::GFP at the wound edge, whereas *Dif dl* cells retain high levels of fluorescence. (*I*) Schematic representation of the wound-edge membranes (green lines) and AJs (blue lines) used for the measurements and quantification of E-cad::GFP fluorescence shown in *J* and *K*. (*J*) Ratio of E-cad::GFP at wound-edge membranes versus E-cad::GFP at AJs away from the wound in wild type and in *Dif dl*. In wild type, this ratio is significantly lower (0.685 ± 0.050) than in *Dif dl* (1.133 ± 0.076), $P = 2.7 \times 10^{-5}$ (Mann–Whitney test). Error bars are SEM. (*K*) E-cad::GFP fluorescence intensity at the membranes surrounding the wound in wild type and in *Dif dl*. Compared with wild type, *Dif dl* embryos show significantly higher E-cad::GFP fluorescence ($P = 9.7 \times 10^{-19}$, Mann–Whitney test). The value in *Dif dl* (15.13 ± 1.136) is nearly fourfold higher than in wild type (3.872 ± 0.318). Measurements of 92 wound-edge membranes from 6 wild-type embryos and 91 wound-edge membranes from 5 *Dif dl* embryos are plotted. Error bars represent SEM. (*L*) Wound closure dynamics in wild-type embryo expressing E-cad::GFP. Images are single time points from *Movie S1*. The initial wound of $2,795 \mu\text{m}^2$ closes rapidly and at 90 min after wounding (minpw), the remaining gap (outlined with a dashed line) is 15-fold smaller: $198.3 \mu\text{m}^2$. (*M*) Wound closure dynamics in *Dif dl* embryo expressing E-cad::GFP. Images are single time points from *Movie S3*. The initial wound of $2,750 \mu\text{m}^2$ remains open and at 90 min minpw is approximately $2,157.5 \mu\text{m}^2$, which is only a 1.3-fold reduction in gap size. (Scale bars: *A*, *E*, *I*, *L*, and *M*, 20 μm ; *B–D* and *F–H*, 5 μm .)

wound-edge cells, whereas E-cad::GFP remained high in *Dif dl* (Fig. 3 *D* and *H*, red dashed lines mark the edge).

We quantified the fluorescence intensity of E-cad::GFP using the Fiji software for image processing and analysis (28). We calculated the ratio of measured fluorescence of each individual wound-edge membrane (Fig. 3*I*, marked in green) to the average fluorescence of parallel AJs that do not contact the wound (Fig. 3*I*, marked in blue), in wild type ($n = 92$) and in *Dif dl* ($n = 91$). The results (Fig. 3*J*) showed that in wild type, that ratio was 0.685 ± 0.051 , whereas in *Dif dl*, it was close to 1 (1.133 ± 0.076). Thus, *Dif dl* mutants failed to down-regulate E-cad::GFP at the wound margin. Similar analysis showed that like *Dif dl*, *Toll*^{-/-} mutants were also inefficient in removing E-cad::GFP from wound-edge membranes (Fig. S2).

We observed two other important features of E-cad::GFP in *Dif dl* mutants. First, the amount of E-cad::GFP was generally higher in *Dif dl* mutants both in wound-edge cells and in cells that were away from the wound (Fig. 3, compare *A* to *E*). The most striking difference in E-cad::GFP fluorescence between wild-type and *Dif dl* epidermal cells was at the membranes that faced the wound directly and that would later assemble the actin cable (Fig. 3*I*, marked in green). Wound-edge membranes in *Dif dl* ($n = 91$) displayed robust E-cad::GFP fluorescence that was nearly fourfold the intensity seen in wild type ($n = 92$) (Fig. 3*K*, $P = 9.7 \times 10^{-19}$). Second, wounds in *Dif dl* showed asymmetry in E-cad::GFP distribution: One side of the wound had stable E-cad::GFP at the wound margin, whereas E-cad::GFP was down-regulated on the opposite side of the wound (Fig. 3*E*). At 5 min after wounding, 63.3% of the imaged *Dif dl* embryos ($n = 30$) displayed asymmetric E-cad::GFP, whereas only 7.7% of the control embryos ($n = 13$) showed this pattern. The apparent asymmetry could result from a partial remodeling of E-cad::GFP in a subset of the wound-edge cells.

Time-lapse imaging until completion of wound closure confirmed that epidermal cells in control embryos ($n = 5$) came together in a symmetric fashion (Fig. 3*L*). At 90 min after ablation, wounds that initially measured approximately $2,800 \mu\text{m}^2$ were in the final stages of closure, shrinking approximately 15-fold in size (Fig. 3*L* and Movie S1). Remarkably, wounds in 57% of *Dif dl* embryos ($n = 7$) maintained asymmetries for the duration of the imaging. At 90 min after ablation, wounds of approximately $2,800 \mu\text{m}^2$ remained open, showing a minimal reduction in size of approximately 1.3-fold (Fig. 3*M* and Movie S3).

Thus, Toll/NF- κ B signaling guides rapid junctional remodeling and uniform movement of epidermal cells immediately after injury.

***Dif* and *dl* Regulate the Turnover of E-Cadherin in *Drosophila* Epidermis.**

Although properly localized, both the endogenous E-cadherin and E-cad::GFP were accumulated to a higher level in both wounded (Fig. 2 compare *F* and *H* to *B*; Fig. 3 compare *A* to *E*) and unwounded *Dif dl* and *Toll*^{-/-} epidermal cells (Figs. S3 and S4). Western blot analysis of *Dif dl* unwounded embryos showed approximately 1.7-fold increase in the amount of E-cad compared with controls (Fig. S5).

These observations led to the hypothesis that Toll/NF- κ B activities promote E-cadherin turnover in normal, unwounded tissue. If this idea were to be true, then mutants lacking NF- κ B activity would accumulate more E-cadherin at the junctions because of inefficient, slow turnover. This defect would be of greater consequence right after wounding when the AJs need to undergo rapid remodeling so that the epidermal cells could proceed with the assembly of actin cable, contraction of the cable, and sealing of the gap.

To test this hypothesis, we used fluorescence recovery after photobleaching (FRAP) of E-cad::GFP to determine the stable fraction present at cell junctions in unwounded epidermis in wild-type (*ubi-E-cad::GFP*+) and in *Dif dl* (*Dif dl ubi-E-cad::GFP*/*Dif dl*+) mutants.

We performed FRAP in the ventral epidermis of embryos at stages 15 and 16. In wild-type embryos, recovery of E-cad::GFP fluorescence was seen as soon as 1 min after bleaching and a very clear signal reappeared at 2 min after bleaching (Fig. 4*A* and Movie S4). At 13 min after bleaching (Fig. 4*A*, Upper), the fluorescence recovery began to reach a plateau (Fig. 4*B*) as reported in an earlier study (29). At that point, approximately 85% of the GFP fluorescence was recovered at the cell membrane, indicating that 15% of E-cad::GFP molecules were in a stable fraction (Fig. 4*B*). Imaging ended at 15 min because our studies pointed to the importance of E-cad::GFP behavior immediately after injury.

By contrast, recovery of E-cad::GFP at bleached cellular interfaces was greatly reduced in *Dif dl ubi-E-cad::GFP* epidermal cells. Although some embryos recovered partial fluorescence at the bleached membrane, we saw no recovery in 31.3% ($n = 16$) of the embryos (Fig. 4*A*, Lower and Movie S5). In *Dif dl*, the stable fraction of E-cad::GFP increased to approximately 60% (Fig. 4*C*). Thus, E-cad::GFP in the epidermis of *Dif dl* embryos was significantly less mobile compared with the pool of E-cad::GFP in wild-type animals ($P = 0.0005$).

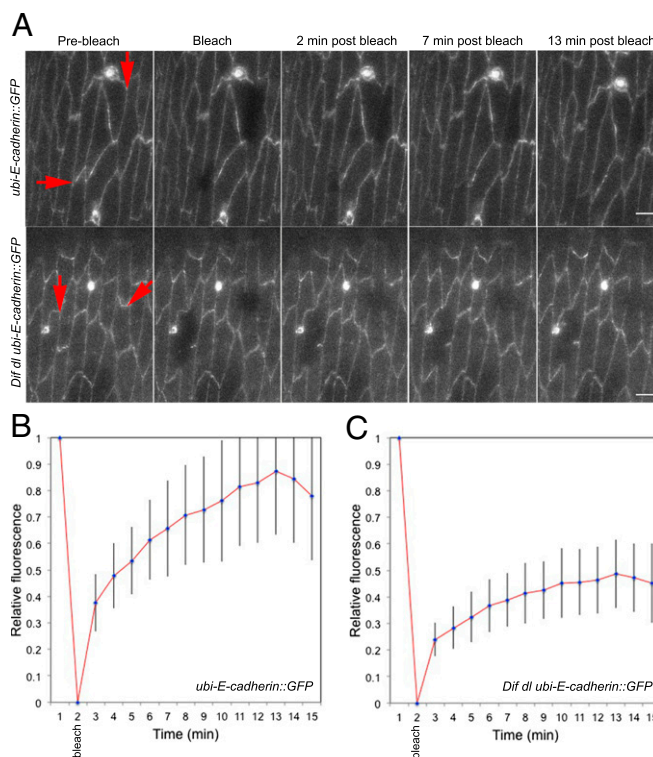


Fig. 4. E-cad::GFP displays slow rate of FRAP in *Dif dl* mutants. Cellular interfaces (arrows) in the ventral and ventral-lateral epidermis of embryos at stage 15–16 expressing E-cad::GFP were photobleached. Images were acquired with identical settings. (*A*, Upper) Time-series images of E-cad::GFP in wild-type embryos (*ubi-E-cad::GFP*+/+). E-cad::GFP recovers rapidly, showing up at the bleached membrane within 2 min after bleaching and reaching approximately 85% recovery at 13 min. (Scale bar: 5 μm .) (*A*, Lower) Time-series images of E-cad::GFP in *Dif dl* embryos (*Dif dl ubi-E-cad::GFP*/*Dif dl* +). No recovery of E-cad::GFP at the cell membrane was seen in 31.3% of the embryos ($n = 16$). (Scale bars: 5 μm .) (*B*) Average fluorescence-recovery kinetics of E-cad::GFP in wild-type embryos ($n = 16$). (*C*) Average fluorescence-recovery kinetics of E-cad::GFP in *Dif dl* embryos ($n = 16$). E-cad::GFP recovery is impaired in *Dif dl* cells: At 13 min after bleaching, only approximately 40% of the fusion protein is present at the bleached cellular interface. Error bars represent SD in *B* and *C*. The recovery curves are significantly different, $P = 0.0005$ (Student's *t* test).

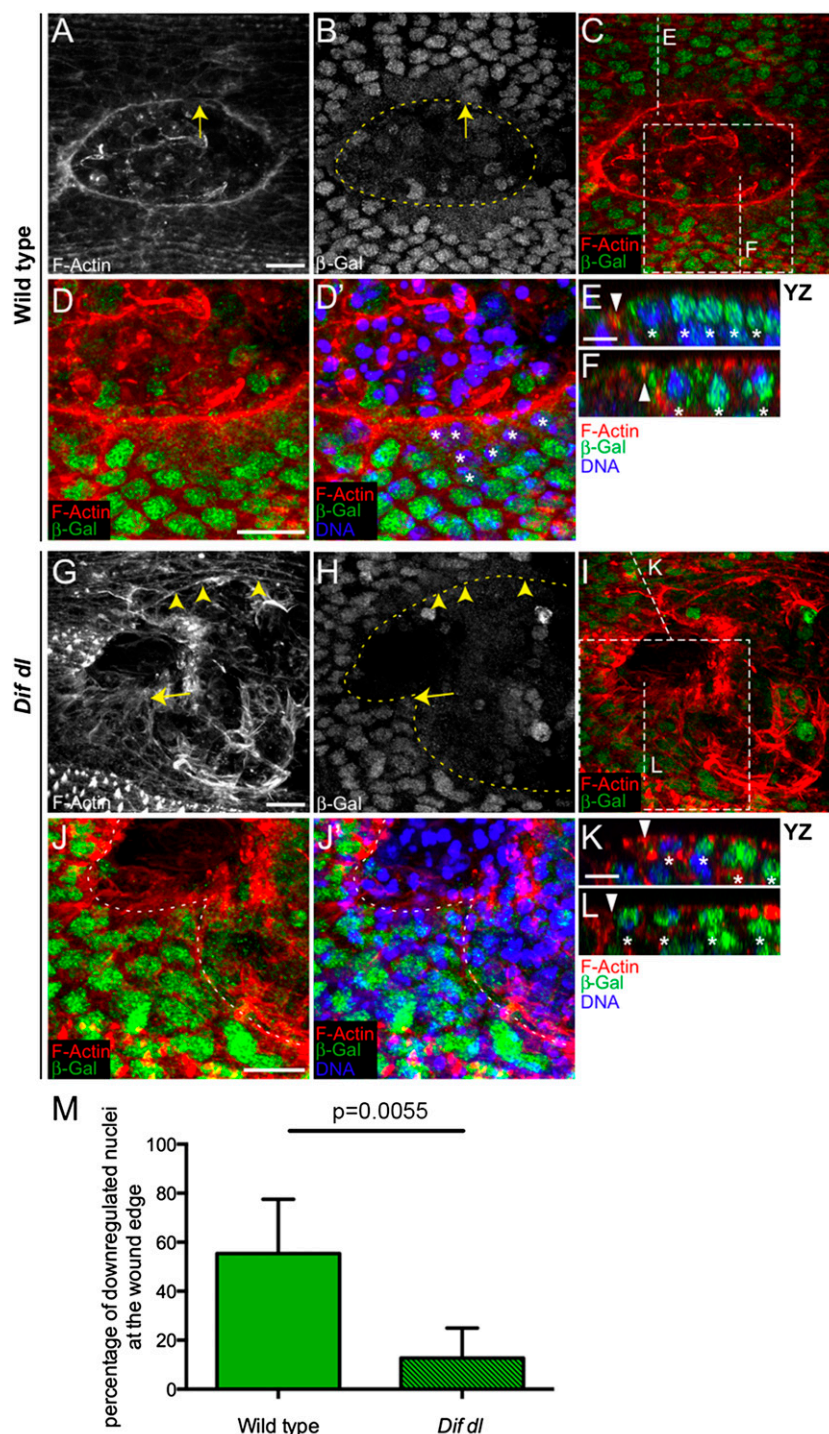


Fig. 6. *Dif* and *Dorsal* are negative regulators of *shotgun* transcription. (A–L) Ventral epidermis of embryos at stage 15 at 1 h after wounding showing F-actin (phalloidin) in red, β -Gal in green, and DNA (DAPI) in blue. β -Gal stains nuclei with active *shotgun* transcription because all embryos are heterozygous for *P(lacW)shg*^{k03401}. Images are the maximum intensity z projections of wild-type (A, B, C, D, and D') and *Dif dl* embryos (G–J') and represent 7.5- to 13- μ m stacks (15–26 slices). D, D', J, and J' represent close-ups of the boxed areas in C and I, respectively. Identical settings were used for all images. In wild type, a continuous actin cable outlines the smooth wound margin (A). In *Dif dl*, the wound edge is irregular and the actin cable is discontinuous (G), with regions showing some actin bundles (arrowheads) and regions showing no actin bundles (arrow). In wild type, the nuclear β -Gal in wound-edge cells is greatly decreased compared with nuclei away from the wound (B–D'). In *Dif dl*, many nuclei at the wound margin maintain high β -Gal expression (H–J'). Nuclei with high levels of β -Gal belong to cells where the actin cable is missing (arrow in G and H). Dashed lines in B, H, J, and J' outline the wound edge. (E, F, K, and L) YZ slices of the regions shown by vertical lines in C and I. Triangles mark the wound edge/actin cable and asterisks mark the epidermal nuclei. The wound is to the left. In wild type, nuclei at the wound edge have a decreased β -Gal compared with nuclei away from the edge (E and F). In *Dif dl*, β -Gal fluorescence is similar in edge and nonedge nuclei where the actin cable is missing (L), but down-regulated in wound-edge nuclei where some actin cable is present (K). (M) Percentage of cells at the wound edge with decreased nuclear β -Gal at 1 h after injury. In wild type, $55.4 \pm 22.2\%$ of the wound-edge cells have decreased nuclear β -Gal, whereas in *Dif dl*, $12.7 \pm 12.3\%$ of the wound-edge cells show β -Gal down-regulation; $P = 0.0055$ (Student's *t* test). Error bars are SD. Five wild-type and five *Dif dl* embryos were quantified. All wound-edge nuclei were measured as follows: 100 wild-type and 83 *Dif dl*. (Scale bars: A–D' and G–J', 10 μ m; E, F, K, and L, 5 μ m.)

in *Dif dl* embryos at 1 h after wounding, a time point when Dorsal was fully translocated to the nuclei of the wound-edge cells (Fig. 5C). As described, the mutant embryos did not have a continuous actin cable; only a few cells showed subtle bundles of F-actin at the wound margin (Fig. 6G, arrowheads). The cells that deposited some actin bundles had lower β -Gal in wound-edge nuclei because of decreased transcription of *shg-lacZ* (Fig. 6K; YZ position shown in Fig. 6I). The cells without an apparent actin cable at the margin (Fig. 6G, arrow) had high nuclear β -Gal fluorescence (Fig. 6H, J, and I; cross-section in Fig. 6L; YZ position shown in Fig. 6I). Counts in five embryos showed that only $12.7 \pm 12.3\%$ of all *Dif dl* epidermal nuclei bordering the wound ($n = 83$) had turned down β -Gal, indicating that the majority of the wound-edge cells did not repress the *shg-lacZ* reporter (Fig. 6M). The difference between wild type and *Dif dl* in regard to the number of nuclei with down-regulated β -Gal was significant ($P = 0.0055$). Therefore, Dif and Dorsal repress *shotgun* transcription in epidermal cells after wounding. In *Dif dl*, the cells that failed to turn down *shotgun* transcription also failed to assemble actin bundles at the wound margin, whereas the cells that had reduced *shotgun* mRNA production assembled actin bundles at the wound margin.

Quantification of *shotgun* mRNA in intact, unwounded *Dif dl* and in control embryos showed that under stress-free conditions, NF- κ B proteins do not repress *shotgun* (Fig. S6). Intact embryos also have very little nuclear Dorsal::GFP (Fig. 5A). However, on wounding, Dorsal::GFP becomes exclusively nuclear around the gap (Fig. 5C) and the *shg-lacZ* reporter is repressed (Fig. 6A–F). Thus, only after strong activation, as in the case of injury, NF- κ B transcription factors repress *shotgun* in epidermal cells.

Discussion

This study describes an essential requirement for the *Drosophila* Toll/NF- κ B pathway in epithelial wound repair. It has been long suspected that failure in epidermal repair would lead both to disruption of the epithelial barrier and to infection, and indeed, *Dif dl* larvae show epidermal gaps and die because of opportunistic infection (8). The experiments revealed that after injury, the Toll/NF- κ B activities in the epidermis control the remodeling and the expression levels of E-cadherin, a crucial component of the AJs; reorganization of the AJs, in turn, is tightly linked to the placement of a thick supramolecular actomyosin cable at the wound margin. It is through these activities that the pathway executes its effect on epidermal repair.

Wound Repair Features Two Levels of E-Cadherin Regulation, both Controlled by the Toll/NF- κ B Pathway. E-cadherin is down-regulated in response to wounding, and this regulation occurs in two sequential, mechanistically distinct, phases. First, the protein is down-regulated at the wound margin within minutes after tissue ablation. We argue that this immediate down-regulation occurs at a posttranscriptional level. The following observations support this conclusion: (i) The decrease in E-cadherin levels is extremely rapid; (ii) down-regulation is seen in embryos that express *E-cad::GFP* under the control of a heterologous (*ubiquitin*) promoter; and (iii) decreased *shotgun* transcription is only evident 1 h after wounding.

We propose that the immediate down-regulation of E-cadherin depends on rapid protein turnover, because E-cadherin turnover has emerged as the primary process governing the steady remodeling of AJs (33). In highly polarized cells, E-cadherin has a half-residence time of only a few minutes at the junction (34) and shuttles continuously between the plasma membrane and the recycling endosomes. The recycling step is controlled in cells that undergo active morphological changes (33). E-cadherin is mobile in the polarized epidermal cells of *Drosophila* late embryos as our FRAP experiments have shown and undergoes rapid reorganization after epidermal injury. Thus, regulation of E-cadherin

trafficking could be important not only for epithelial morphogenesis in *Drosophila* (35) but also for epithelial wound closure.

The second mode of E-cadherin down-regulation is seen at approximately 1 h after wounding and is transcriptional. In cells bordering the wound, the transcription of *shotgun* decreases; this transcriptional repression likely contributes to the sustained down-regulation of E-cadherin around the wound.

Our results show that the Toll/NF- κ B pathway controls both modes of E-cadherin regulation at the wound edge. We envision two separate NF- κ B activities that converge on E-cadherin expression to ensure continuous down-regulation of E-cadherin. In contrast to wild-type embryos, E-cadherin remains at the plasma membrane in wound-edge cells in *Toll^{-/-}* and *Dif dl* embryos. Therefore, NF- κ B activity is required for the early, post-transcriptional down-regulation of E-cadherin. Molecules that control the rate of E-cadherin trafficking directly or regulate F-actin dynamics, which is intertwined with E-cadherin function (36), could be the transcriptional targets of the Toll/NF- κ B pathway. These molecules stimulate E-cadherin turnover both in unwounded and wounded state, but their absence is more apparent in injured embryos where rapid remodeling of the AJs is pivotal for wound closure.

The Toll/NF- κ B pathway also controls the second mode of E-cadherin regulation, transcriptional down-regulation. Although expression of *shotgun* decreases around the wound in wild-type embryos, *shotgun* continues to be expressed at the wound edge in *Dif dl* mutants. Nuclear translocation of Dorsal precedes the transcriptional repression of E-cadherin and occurs simultaneously with the initial, fast down-regulation of E-cadherin at the wound edge. Like other NF- κ B proteins, Dorsal can either be a transcriptional activator or a repressor (37); however, whether *shotgun* is the direct target of Dif and Dorsal remains to be investigated.

Although the lack of E-cadherin at the wound edge was reported (25), its significance was not obvious. Our analysis of *Toll^{-/-}* and NF- κ B mutants provides clear evidence that the dynamics of E-cadherin at the wound edge is regulated and important. We propose that E-cadherin remodeling is linked to actin-bundle assembly and that only the epidermal cells that efficiently turn down E-cadherin are able to place a bundle of actin filaments at the wound edge. Removal of cell adhesion complexes could provide an open space at the wound-edge membrane for actin nucleation, polymerization and immediate subcortical placement of filaments. This distinct domain for contractile F-actin is a direct result of Toll-mediated activities.

The Toll/NF- κ B Pathway as a Stress Response System in the *Drosophila* Epidermis. As the outermost layer of the animal body, the epidermis is in immediate contact with the environment. The epidermal cells survey the surroundings and respond swiftly to abrupt changes. The Toll receptor senses acute stress such as a breach in the epidermis and the NF- κ B transcription factor Dorsal is activated. Together with Dif, Dorsal mounts an immediate response that results in gap closure. We propose that the Toll/NF- κ B module monitors cellular stress continuously and acts as a first responder in the epidermis at all times. The pathway fulfills this function at least in part through its ability to control the junctional complexes in epidermal cells.

Acute stress, including injury, would trigger a response that would consume the available stress-response molecules, which must be replenished. Therefore, a burst of NF- κ B-dependent gene expression would follow an event of intense cellular stress. This burst of NF- κ B activity will restore the diminished stress-response molecules; it could also result in NF- κ B transcriptional activation of new, repair-specific genes or a temporary transcriptional repression of other genes.

The Toll/NF- κ B pathway responds to another type of intense stress caused by microbial infection, and both *Drosophila* larvae and adults rely on the pathway for immune protection (7, 8, 38, 39). If the aim of immune defense is microbial clearance, then

the animal likely employs a different set of NF- κ B targets than the ones used in wound closure. Nevertheless, certain cellular mechanisms could be conserved. For example, macrophages in *Dif dl* larvae fail to phagocytose microbes (8). Defects in F-actin dynamics and in vesicle trafficking because of missing NF- κ B targets could be responsible for the defective phagocytosis.

In mammals, Toll-like receptors (TLRs) are pattern-recognition receptors that recognize directly molecules shared by pathogens. However, TLRs can also bind to host molecules including self DNA, products of the extracellular matrix, and heat-shock proteins, which are released during injury and are considered damage-associated molecular patterns (40). A number of TLRs, NF- κ B proteins, and I κ B family members are expressed in the mammalian epidermis and are essential for epidermal homeostasis (30, 41), but studies on epidermal resealing in mutant mouse lines are lacking.

Following injury, the *Drosophila* Toll is not activated by Spätzle, the ligand that triggers the maternal cascade. This finding opens the possibility that like in mammals, the Toll receptor can recognize directly damage-associated molecular patterns generated during injury and that this recognition would activate the downstream cascade in epidermal cells.

The ability to sense, respond, and adapt to the ever-changing environment is a fundamental quality of life and a remarkably similar molecular pathway that detects aberrations in the environment and provides an inducible regulation of gene expression is in place both in *Drosophila* and in higher vertebrates.

Materials and Methods

***Drosophila* Stocks and Genetics.** Single mutants were of the genotypes: *Toll^{9ORE}/Toll^{1-RXA}* and *spz^{rm7}/spz¹⁹⁷* (42, 43). *Dif dl* mutants were of the genotype *Df(2L)J4/Df(2L)TW119* (8). In all cases, transallelic combinations were used to avoid effects from second site mutations. The *shotgun* allele was *P(lacW)shg^{k03401}* (44). All alleles were crossed to balancer stocks that express GFP under the control of the *twist* promoter (45). Mutant embryos were identified by the absence of GFP fluorescence.

Second-chromosome insertions of *ubi-E-cad::GFP* (26), *sqh-Gap43::mCherry* (27), *sqh-sqh::GFP* (46), and *P(lacW)shg^{k03401}* were recombined onto a *Dif dl* chromosome; third chromosome insertion of *sqh-Gap43::mCherry* was recombined onto a *Toll^{9ORE}* chromosome. *UAS-CherryFP::Moesin* under the control of *e22C-Gal4* (47) was used to visualize F-actin in Movie S2.

In rescue experiments, the *dl::GFP* transgene was crossed into a *Dif dl* mutant background. Survival to adulthood in percents was determined by comparing the number of *Dif dl* mutants that carried *dl::GFP* to the number of *Dif dl/+* heterozygous siblings from the same cross (defined as 100%).

Wounding Assay. Embryos were collected from laying pots kept at 25 °C overnight, dechorionated in 50% bleach and rinsed extensively with water. Because mutants were balanced with GFP-expressing balancer chromosomes, non-GFP embryos of stages 15 and 16 were selected under UV light. Embryos were staged as described (48). Mutant embryos were aligned on a slide that already had a piece of double-sided tape affixed to it. The embryos were then covered with halocarbon oil 700 (Sigma) and a coverslip, and wounded by using a nitrogen laser-pumped dye laser (Micropoint Photonic Instruments) connected to an Andor Revolution Spinning Disk Confocal Microscope (Andor Technology). After wounding, the coverslip was removed carefully and the embryos were left to recover in a humid chamber at 20 °C. The wounded embryos were scored under a dissecting microscope for wound closure 16 h later. Percentage of wound closure was calculated as the ratio of nearly hatching embryos with unclosed wounds over the total number of wounded embryos (dead animals were excluded).

Immunohistochemistry. Embryos of early stage 15 were wounded and placed in a humid chamber to recover. Wounded embryos were transferred to a glass vial containing a mix of 1:1 heptane and 8% (vol/vol) formaldehyde in PBS [or 4% (wt/vol) freshly made paraformaldehyde] and fixed for 40 min. Embryos were removed from the fixative, manually devitellinized, and incubated for 4 h in a blocking solution (1% BSA in PBSTT, which is 0.1% Triton X-100 and 0.1% Tween-20 in PBS) and then overnight with the primary antibody. The primary antibodies and probes used were the following: 1:50 rat E-cadherin (Developmental Studies Hybridoma Bank), 1:2,500 rabbit β -Gal (Cappel), 1:500 mouse GFP (Invitrogen), 1:200 phalloidin (Invitrogen), and 1 μ g/mL DAPI (Sigma). Following incubation, embryos were rinsed and

washed for 1 h in PBSTT, incubated for 2 h with secondary antibodies conjugated to Alexa-488 or Alexa-568 (Invitrogen), washed in PBSTT, and mounted in 80% (vol/vol) glycerol, 2% (wt/vol) DABCO (Sigma). Imaging was performed on a Zeiss LSM 710 Confocal Microscope with a Zeiss 63 \times Plan Apochromat N.A. 1.4 objective.

Live Imaging. Dechorionated embryos were mounted on glass-bottom culture dishes (MatTek) and covered with halocarbon oil 27 (Sigma). Time-lapse microscopy of E-cad::GFP and Dorsal::GFP was performed in embryos at 25 °C on the Andor Revolution Spinning Disk Confocal Microscope (Andor) with a Nikon 60 \times Plan Apo VC PFS N.A. 1.4 objective. Individual z slices with a step size of 0.4 μ m were taken every 5 min for 180–200 min.

For live imaging of E-cad::GFP and membrane::mCherry upon wounding, embryos were imaged 5 min after laser ablation on a Zeiss LSM 710 Confocal Microscope with a Zeiss 63 \times Plan Apochromat N.A. 1.4 objective. Individual z slices with a step size of 0.4 μ m were processed with Fiji.

Quantification of E-cad::GFP Fluorescence. Maximum projections of stacks of 28–34 confocal z slices (11–13 μ m) captured 5 min after laser ablation of embryos expressing *ubi-E-cad::GFP* were used. Control and *Dif dl* embryos were imaged with identical settings. Nonspecific fluorescence originating from the vitelline membrane was eliminated by using a custom MATLAB script. Fluorescence levels of E-cad::GFP were measured with Fiji. Analysis of the membrane::mCherry channel confirmed the wound edge. Fluorescence measurements were done of all wound-edge cell membranes (10–23 per embryo) and in parallel AJs at least six rows away from the wound margin (5–38 junctions per embryo). Background fluorescence was subtracted from the measured values. Measurements of 92 wound-edge membranes in six wild-type embryos and 91 wound-edge membranes in five *Dif dl* were analyzed for the graphs shown in Fig. 3 J and K. Mann–Whitney test was applied when evaluating statistical significance.

To obtain fluorescence intensity ratios (Fig. 3J), the average fluorescence of AJs that were away from the wound but parallel to the wound margin was calculated for each embryo; the fluorescence value for each wound-edge membrane was then divided by this average value of distant AJs for each embryo. For the quantifications shown in Fig. 3K, average fluorescence intensity was measured at the wound margin in wild type and in *Dif dl*.

Quantification in *Toll^{1-RXA}* was done in a similar way (Fig. S2). Results represent measurements of 68 junctions in five wild-type embryos and 99 junctions in six *Toll^{1-RXA}* embryos.

Quantification of *shotgun-lacZ* Expression. Analysis of *shg-lacZ* expression was performed on heterozygous embryos (*shg^{k03401}/+*) at 1 h after wounding. Fixed and stained embryos in which the actin cable was formed but contraction had not begun were chosen for quantification. Nuclear β -Gal fluorescence was measured in five wild-type and five *Dif dl* embryos; the measurements reflect the analysis of 100 wound-edge nuclei in total in wild type and 83 wound-edge nuclei in *Dif dl*. Student's *t* test was used to test for significant differences between genotypes.

In quantifications, cell nuclei were selected based on the DAPI staining, and the mean fluorescence intensity of β -Gal was measured with Fiji. Values of wound-edge nuclei were normalized by dividing the fluorescence measurement obtained for each nucleus by the average fluorescence value of four nuclei located six rows away from the wound. Fluorescence in wound-edge nuclei was considered down-regulated when its value was below a set threshold: the arithmetic mean of β -Gal fluorescence measurements of 100 wild-type wound-edge nuclei.

FRAP Analysis. Embryos were aged at 25 °C, dechorionated in 50% bleach, rinsed with water, mounted on glass-bottom chambers (MatTek), and covered with halocarbon oil 700 (Sigma). FRAP experiments were done on a Zeiss LSM 510 META laser-scanning confocal microscope using a Plan Apochromat 63 \times /N.A. 1.4 objective. A region of interest (ROI) defined close to the cell membrane was photobleached and monitored for fluorescence recovery over time. A set of 15 images was acquired at an interval of 1 min. Fluorescence recovery was analyzed by measuring the mean gray value within the ROI using Fiji. The ROI was adjusted in each individual image manually to correct for slight movements in the epidermis. To create the fluorescence recovery curve, the background-corrected fluorescence intensities were transformed into a 0–1 scale.

Western Blot Analysis and Quantitative PCR. A description is provided in the *SI Materials and Methods*.

ACKNOWLEDGMENTS. We thank J. Rino, A. Temudo, and T. Pereira for advice on imaging and MATLAB scripts; R. DeLotto for the *dl::GFP* transgene; A. Martin and M. Tworoger for the *Gap43::mCherry* flies; DSHB for the E-cadherin antibody; the Bloomington Stock Center for *Drosophila* shipments;

and Kathryn Anderson and Dennis Diener for comments on the manuscript. Our research was supported by Fundação para a Ciência e a Tecnologia, Portugal (to N.M.), Marie Curie Fellowship PIEF-GA-2009-255573 (to L.C.), and European Research Council Grant 2007-StG-208631 (to A.J.).

- Martin P, Lewis J (1992) Actin cables and epidermal movement in embryonic wound healing. *Nature* 360(6400):179–183.
- Kiehart DP, Galbraith CG, Edwards KA, Rickoll WL, Montague RA (2000) Multiple forces contribute to cell sheet morphogenesis for dorsal closure in *Drosophila*. *J Cell Biol* 149(2):471–490.
- García-Fernández B, Campos I, Geiger J, Santos AC, Jacinto A (2009) Epithelial re-sealing. *Int J Dev Biol* 53(8–10):1549–1556.
- Schäfer M, Werner S (2007) Transcriptional control of wound repair. *Annu Rev Cell Dev Biol* 23:69–92.
- Mace KA, Pearson JC, McGinnis W (2005) An epidermal barrier wound repair pathway in *Drosophila* is mediated by *rainy head*. *Science* 308(5720):381–385.
- Ting SB, et al. (2005) A homolog of *Drosophila rainy head* is essential for epidermal integrity in mice. *Science* 308(5720):411–413.
- Matova N, Anderson KV (2010) *Drosophila* Rel proteins are central regulators of a robust, multi-organ immune network. *J Cell Sci* 123(Pt 4):627–633.
- Matova N, Anderson KV (2006) Rel/NF- κ B double mutants reveal that cellular immunity is central to *Drosophila* host defense. *Proc Natl Acad Sci USA* 103(44):16424–16429.
- Moussian B, Roth S (2005) Dorsoventral axis formation in the *Drosophila* embryo—shaping and transducing a morphogen gradient. *Curr Biol* 15(21):R887–R899.
- Morisato D, Anderson KV (1994) The *spätzle* gene encodes a component of the extracellular signaling pathway establishing the dorsal-ventral pattern of the *Drosophila* embryo. *Cell* 76(4):677–688.
- Schneider DS, Jin Y, Morisato D, Anderson KV (1994) A processed form of the *Spätzle* protein defines dorsal-ventral polarity in the *Drosophila* embryo. *Development* 120(5):1243–1250.
- Belvin MP, Jin Y, Anderson KV (1995) Cactus protein degradation mediates *Drosophila* dorsal-ventral signaling. *Genes Dev* 9(7):783–793.
- Roth S, Stein D, Nüsslein-Volhard C (1989) A gradient of nuclear localization of the dorsal protein determines dorsoventral pattern in the *Drosophila* embryo. *Cell* 59(6):1189–1202.
- Steward R (1989) Relocalization of the dorsal protein from the cytoplasm to the nucleus correlates with its function. *Cell* 59(6):1179–1188.
- Leptin M (2005) Gastrulation movements: The logic and the nuts and bolts. *Dev Cell* 8(3):305–320.
- Ip YT, Gridley T (2002) Cell movements during gastrulation: Snail dependent and independent pathways. *Curr Opin Genet Dev* 12(4):423–429.
- Gerttula S, Jin YS, Anderson KV (1988) Zygotic expression and activity of the *Drosophila Toll* gene, a gene required maternally for embryonic dorsal-ventral pattern formation. *Genetics* 119(1):123–133.
- Hashimoto C, Gerttula S, Anderson KV (1991) Plasma membrane localization of the Toll protein in the syncytial *Drosophila* embryo: Importance of transmembrane signaling for dorsal-ventral pattern formation. *Development* 111(4):1021–1028.
- Patterson RA, et al. (2013) Serine proteolytic pathway activation reveals an expanded ensemble of wound response genes in *Drosophila*. *PLoS ONE* 8(4):e61773.
- Ip YT, et al. (1993) *Dif*, a dorsal-related gene that mediates an immune response in *Drosophila*. *Cell* 75(4):753–763.
- Stein D, Goltz JS, Jurcsak J, Stevens L (1998) The Dorsal-related immunity factor (*Dif*) can define the dorsal-ventral axis of polarity in the *Drosophila* embryo. *Development* 125(11):2159–2169.
- Payre F (2004) Genetic control of epidermis differentiation in *Drosophila*. *Int J Dev Biol* 48(2–3):207–215.
- Campos I, Geiger JA, Santos AC, Carlos V, Jacinto A (2010) Genetic screen in *Drosophila melanogaster* uncovers a novel set of genes required for embryonic epithelial repair. *Genetics* 184(1):129–140.
- Wood W, et al. (2002) Wound healing recapitulates morphogenesis in *Drosophila* embryos. *Nat Cell Biol* 4(11):907–912.
- Abreu-Blanco MT, Verboon JM, Liu R, Watts JJ, Parkhurst SM (2012) *Drosophila* embryos close epithelial wounds using a combination of cellular protrusions and an actomyosin purse string. *J Cell Sci* 125(Pt 24):5984–5997.
- Oda H, Tsukita S (2001) Real-time imaging of cell-cell adherens junctions reveals that *Drosophila* mesoderm invagination begins with two phases of apical constriction of cells. *J Cell Sci* 114(Pt 3):493–501.
- Martin AC, Gelbart M, Fernandez-Gonzalez R, Kaschube M, Wieschaus EF (2010) Integration of contractile forces during tissue invagination. *J Cell Biol* 188(5):735–749.
- Schindelin J, et al. (2012) Fiji: An open-source platform for biological-image analysis. *Nat Methods* 9(7):676–682.
- Oshima K, Fehon RG (2011) Analysis of protein dynamics within the septate junction reveals a highly stable core protein complex that does not include the basolateral polarity protein Discs large. *J Cell Sci* 124(Pt 16):2861–2871.
- Wullaert A, Bonnet MC, Pasparakis M (2011) NF- κ B in the regulation of epithelial homeostasis and inflammation. *Cell Res* 21(1):146–158.
- DeLotto R, DeLotto Y, Steward R, Lippincott-Schwartz J (2007) Nucleocytoplasmic shuttling mediates the dynamic maintenance of nuclear Dorsal levels during *Drosophila* embryogenesis. *Development* 134(23):4233–4241.
- Jezowska B, et al. (2011) A dual function of *Drosophila* capping protein on DE-cadherin maintains epithelial integrity and prevents JNK-mediated apoptosis. *Dev Biol* 360(1):143–159.
- Trojanovsky SM (2009) Regulation of cadherin-based epithelial cell adhesion by endocytosis. *Front Biosci (Schol Ed)* 1:61–67.
- de Beco S, Gueudry C, Amblard F, Coscoy S (2009) Endocytosis is required for E-cadherin redistribution at mature adherens junctions. *Proc Natl Acad Sci USA* 106(17):7010–7015.
- Wirtz-Peitz F, Zallen JA (2009) Junctional trafficking and epithelial morphogenesis. *Curr Opin Genet Dev* 19(4):350–356.
- Michael M, Yap AS (2013) The regulation and functional impact of actin assembly at cadherin cell-cell adhesions. *Semin Cell Dev Biol* 24(4):298–307.
- Rusch J, Levine M (1996) Threshold responses to the dorsal regulatory gradient and the subdivision of primary tissue territories in the *Drosophila* embryo. *Curr Opin Genet Dev* 6(4):416–423.
- Lemaître B, Nicolas E, Michaut L, Reichhart JM, Hoffmann JA (1996) The dorsoventral regulatory gene cassette *spätzle/Toll/cactus* controls the potent antifungal response in *Drosophila* adults. *Cell* 86(6):973–983.
- Meng X, Khanuja BS, Ip YT (1999) Toll receptor-mediated *Drosophila* immune response requires *Dif*, an NF- κ B factor. *Genes Dev* 13(7):792–797.
- Chen GY, Nuñez G (2010) Sterile inflammation: Sensing and reacting to damage. *Nat Rev Immunol* 10(12):826–837.
- Miller LS (2008) Toll-like receptors in skin. *Adv Dermatol* 24:71–87.
- Tearle R, Nüsslein-Volhard C (1987) Tübingen mutants and stocklist. *Drosoph Inf Serv* 66:209–269.
- Anderson KV, Jürgens G, Nüsslein-Volhard C (1985) Establishment of dorsal-ventral polarity in the *Drosophila* embryo: Genetic studies on the role of the *Toll* gene product. *Cell* 42(3):779–789.
- Tepass U, et al. (1996) *shotgun* encodes *Drosophila* E-cadherin and is preferentially required during cell rearrangement in the neuroectoderm and other morphogenetically active epithelia. *Genes Dev* 10(6):672–685.
- Halfon MS, et al. (2002) New fluorescent protein reporters for use with the *Drosophila* Gal4 expression system and for vital detection of balancer chromosomes. *Genesis* 34(1–2):135–138.
- Royou A, Field C, Sisson JC, Sullivan W, Karsenti R (2004) Reassessing the role and dynamics of nonmuscle myosin II during furrow formation in early *Drosophila* embryos. *Mol Biol Cell* 15(2):838–850.
- Millard TH, Martin P (2008) Dynamic analysis of filopodial interactions during the zipper phase of *Drosophila* dorsal closure. *Development* 135(4):621–626.
- Campos-Ortega JA, Hartenstein V (1985) *The Embryonic Development of Drosophila Melanogaster* (Springer, Berlin).